In situ Carbon Isotopic Exploration of an Active Submarine Volcano

Anna P. M. Michel*^, Department of Applied Ocean Physics and Engineering, Woods Hole Oceanographic Institution, Woods Hole, Massachusetts 02543
amichel@whoi.edu

Scott D. Wankel*^, Department of Marine Chemistry and Geochemistry, Woods Hole Oceanographic Institution, Woods Hole, Massachusetts 02543
sdwankel@whoi.edu

Jason Kapit, Department of Applied Ocean Physics and Engineering, Woods Hole Oceanographic Institution, Woods Hole, Massachusetts 02543

Zoe Sandwith, Department of Marine Chemistry and Geochemistry, Woods Hole Oceanographic Institution, Woods Hole, Massachusetts 02543

Peter R. Girguis, Department of Organismic and Evolutionary Biology, Harvard University, Cambridge, Massachusetts 02138

Abstract:
The geologic and biogeochemical cycling of carbon in deep ocean environments has important implications for our understanding of the functioning of Earth systems across a wide range of spatial and temporal scales. To improve our ability to study the cycling and fluxes of carbon in the deep ocean, new technologies are emerging for making *in situ* measurements of carbon compounds over a range of environmental contexts. Within many of these deep-sea environments, fluxes of carbon compounds often occur as either venting fluids or rising gas bubbles. Key compounds of interest include methane (CH_4), dissolved inorganic carbon (DIC), and carbon dioxide (CO_2) – a component of DIC. In particular, measurement of the carbon isotopic composition ($\delta^{13}C$) of these pools can offer a better understanding of the nature of sources, fluxes, and cycling processes involving these compounds. Here we present the advancement of an *in situ* laser spectrometer (initially developed for measurement of $\delta^{13}C_{CH4}$ only) into a sensor that can measure $\delta^{13}C$ of both CH_4 and CO_2 in both deep-sea bubble plumes as well as geologic fluids. We present results of a 2014 investigation of a back arc submarine volcano (Kick'em Jenny) in the Caribbean Sea. *In situ* isotopic analysis of both bubbles and fluids suggest a primarily thermogenic origin for CH_4 and a magmatic origin for CO_2, yet highlight the occurrence of some heterogeneities indicating locally elevated contribution of organic matter to DIC fluxes.

Keywords: laser spectroscopy; deep-sea instrumentation; carbon isotopes; methane; carbon dioxide; back arc volcano; Kick'em Jenny; E/V Nautilus; Cruise ID NA054

* Corresponding author; ^authors contributed equally

© 2017. This manuscript version is made available under the Elsevier user license
http://www.elsevier.com/open-access/userlicense/1.0/

1. Introduction

The cycling of carbon in deep marine environments reflects the combined influences of a broad range of physical, geological and biological processes manifested across a range of spatial and temporal scales. At the tectonic scale, subduction zones represent key boundaries at which ocean crust is recycled through the mantle – with implications for carbon burial and release on geologic timescales. Depending on the location, burial of this ocean crust removes large amounts of carbon as both carbonate-rich sediments and as buried organic matter. Eventually these pools of carbon can be released as carbon dioxide (CO_2)-rich hydrothermal fluids through submarine back arc volcanic activity. These vigorously rising fluids associated with submarine arc volcanism act to promote hydrothermal circulation through overlying sediments, often stimulating chemosynthetic ecosystems through the delivery of energy-rich fluids containing variable levels of methane and sulfide. The interplay of hydrothermal fluid circulation and biogeochemical reactions supported by these ecosystems may in turn play important roles in regulating the submarine release of these climatically active gases. Thus, understanding the cycling of carbon in the deep sea has implications for Earth systems at many scales, shedding light on the nature of life under extreme conditions and on key carbon transfer processes in these seafloor ecosystems.

In order to further our understanding of the dynamics of carbon release and cycling in the deep sea, there is a need for expanding the temporal and spatial resolution of measurements – and thus, for developing new technologies that can operate under the extreme conditions imposed by the deep sea. As advances in chemical sensor technologies progress, the underwater adaptation of these approaches yields new opportunities for making chemical and isotopic measurements, and for revealing new aspects and characteristics of the deep sea. Among the most rapidly advancing sensing modalities in development for underwater application is infrared laser spectroscopy. Infrared laser-based sensing has been used for optical gas measurements in applications ranging from atmospheric science to medical analyses (e.g. Hodgkinson and Tatam, 2012; Martin 2002; McCurdy et al. 2007; Sigrist et al. 2012; Tittel et al. 2013). Laser-based spectroscopic sensors are highly sensitive and precise, and through wavelength specificity allow application to a wide range of gases, many of which are important for ocean studies (e.g. CO_2, methane (CH_4), and nitrous oxide (N_2O)). Such sensors have also proven effective for stable isotopic measurements including those of carbon, hydrogen, nitrogen and oxygen isotopes (e.g. Baer et al, 2002; Jost et al. 2006; Kosterver et al 1999; Lis et al. 2008; Penna et al. 2010; Waechter and Sigrist 2007; Wahl et al. 2006; Weidmann et al. 2005). Central to adaptation of these laser-based platforms is the ability to efficiently extract dissolved gases from fluids under the high pressure of the deep sea. Towards this end, a variety of high-pressure membrane inlets have been developed for *in situ* analysis of dissolved gases (e.g. Bell et al. 2007; Camilli, and Duryea, 2009; Camilli and Hemond, 2004;

Fietzek et al. 2009; Graziani et al 2014; Hemond and Camilli, 2002; Wankel et al., 2010).

Previously, a deep-sea near-infrared laser spectrometer coupled to a membrane inlet for gas extraction was designed and field-tested in Monterey Bay, CA (Wankel et al. 2013). This *in situ* laser spectrometer was designed to measure methane carbon isotopic composition ($\delta^{13}C_{CH4}$) at depths up to 3000 m, and was successfully deployed to a depth of 960 m for investigation of $\delta^{13}C_{CH4}$ variations at cold seep environments. While this study demonstrated the successful application of such instrumentation to study a biogeochemically active seafloor habitat, analyses were limited to the $\delta^{13}C_{CH4}$ analysis of fluids. This measurement, along with assumptions about microbial isotopic fractionation, allowed the investigators to make geo-referenced estimates of the net anaerobic methane oxidation in the subsurface, without relying on the collection and analyses of numerous sediment samples on board ship. However, understanding the fate of methane-derived carbon benefits tremendously from coupling $\delta^{13}C_{CH4}$ measurements to $\delta^{13}C_{CO2}$ measurements. Indeed, well-established methods of studying carbon cycling via the analyses of many discrete samples routinely demonstrate the occurrence of processes (e.g., methane oxidation or organic matter pyrolysis) by co-examination of $\delta^{13}C_{CO2}$ and $\delta^{13}C_{CH4}$. Here we present a newly advanced deep-sea laser spectrometer capable of *in situ* analyses of both CH_4 and CO_2 carbon isotopes. We demonstrate its novel capacity to make *in situ* measurements of both fluid and gas samples, facilitating the study of gas/fluid equilibrium processes at *in situ* conditions. These developed capabilities are detailed in the context of a teleprescence-enabled expedition devoted to the investigation of an active submarine volcano, Kick'em Jenny (KEJ), using the remotely operated vehicle (ROV) *Hercules* and the E/V *Nautilus* (Bell et al. 2015).

2. Instrument Design and Configuration

2.1 Overview of First Generation Laser Spectrometer

Development of the first generation deep-sea laser spectrometer has been detailed previously (Wankel et al. 2013) for *in situ* quantification of $\delta^{13}C_{CH4}$ in the deep sea. This instrument utilizes off-axis integrated cavity output spectroscopy (ICOS) with a near-infrared laser having a wavelength of 1647 nm for methane detection. Laser current tuning allows for coverage from 1647.5 nm to 1648.1 nm, a region containing spectral peaks for $^{12}C_{CH4}$ and $^{13}C_{CH4}$ as well as $^{12}CO_2$. Dissolved CH_4 was extracted from seawater through the use of a flow-through, high-pressure membrane inlet in which dissolved gases are extracted from seawater through a thin semi-permeable Teflon AF membrane (Wankel et al. 2010). The developments detailed below largely involve modifications to this pre-existing instrument as well as external features for expansion of sampling capabilities.

2.2 Added Capabilities of the New Laser Spectrometer

The laser spectrometer was designed to incorporate two lasers (each at a distinct wavelength for targeting specific gases) passing through a single optical cavity (operated at a reduced pressure of 10 torr) with light from both lasers collected by a single detector. For measurement of carbon isotopes of CO_2, a second laser (1602 nm) was also incorporated. By current tuning this laser, we targeted isotopic peaks of CO_2 between 1602.4 nm and 1602.7 nm. This wavelength region includes spectral peaks for $^{12}CO_2$, $^{13}CO_2$, $C^{18}O^{16}O$, (and H_2S) as described below.

While the first-generation membrane inlet system (Wankel et al. 2013; Wankel et al., 2011) was designed to extract dissolved gases from seawater, we developed a second-generation extractor that can analyze the gas composition of bubbles emanating from the seafloor. During sampling of dissolved gases, seawater is passed directly across the semi-permeable Teflon (Teflon AF 2400; Biogeneral, Inc.) – allowing dissolved gases to diffuse across the membrane into the analyzer. This membrane serves to separate the high-pressure seawater environment from the internal analyzer, which operates at atmospheric pressure. To increase the transfer efficiency of dissolved gases through the membrane, the membrane surface area was increased from ~2cm^2 to an area of 13.4cm^2, representing an increase by a factor of ~7. The larger surface area Teflon membrane has a thickness of 37μm and was physically supported by a porous stainless steel frit (5 μm pore size). For analysis of bubbles, aliquots of gas were similarly passed directly across this membrane. The inlet flow orientation was also changed from a ninety-degree flow configuration to one where the inlet and outlet are perpendicular to the membrane – with no noticeable change in response. The pressure bearing strength of the membrane was regularly confirmed prior to deployment by pressurization to 5000 psi using a handheld pump (Druck, Inc.).

It has been previously noted that considerable isotopic fractionation of CH_4 occurs during extraction through the membrane inlet (Wankel et al. 2013). Fluid flow rate plays the largest role in regulating the offset between true and measured isotopic values (not temperature and hydrostatic pressure). At a constant flow rate this artifact can be empirically corrected (Wankel et al. 2013). Here we conducted new laboratory experiments to similarly determine the dynamics of carbon isotopic fractionation for CO_2 transfer across the membrane (from acidified seawater). To this end, we performed experiments using the same membrane inlet attached to a laboratory based ICOS Carbon Dioxide Isotope analyzer (Los Gatos Research: CCIA-43EP, mid-infrared laser spectrometer). Briefly, seawater flow was directed past the membrane at a range of rates, with permeated sample gases delivered to the analyzer using a sweep gas. As the dynamics of gas permeation at the membrane interface are independent of the analyzer, the use of the benchtop analyzer allowed for a more efficient evaluation of the effects of flow rate on carbon isotopic fractionation.

2.3 ROV Integration, pumping, plumbing and sampling modes

The laser spectrometer was housed in a 6AL-4V titanium pressure vessel and integrated onto the ROV *Hercules*. The ROV provided 24 VDC power and Ethernet communications to the laser spectrometer via deep-sea connectors (SubConn, Inc.). The laser spectrometer had a total power draw of approximately 70W. The ROV was equipped with additional sensors providing temperature data (on board temperature probe) and water depth.

During deployments, a fluid pumping and plumbing system was installed on the ROV to deliver sample fluids and gas bubbles to the membrane inlet of the laser spectrometer for analysis. A schematic of the sampling configuration is detailed in Figure 1. This system operated in two modes: fluid sampling and bubble sampling. To switch between the two modes, a three-way valve (Swagelok, Inc.) located on the front of the ROV was manually operated using the ROV manipulator. In both modes, a deep-sea impeller pump (SBE 5M; SeaBird, Inc.) was placed downstream of the membrane inlet acting to pull sample fluids or bubbles past the membrane inlet.

In fluid mode, the ROV manipulator positioned a sampling wand into target fluids and dissolved gases were extracted into the instrument through the membrane as described above for analysis of CH_4 and/or CO_2. In general, at the flow rates used, this approach acts to extract dissolved CO_2 but depending on pH does not account for the speciation of all carbonate species (including carbonate and bicarbonate). For explicit measurement of the $\delta^{13}C$ of the total dissolved inorganic carbon (DIC) pool, the seawater sample stream was acidified to a pH < 3 shifting the speciation of the DIC pool to 99.9% CO_2. Inline acidification was conducted by addition of small amounts of concentrated acid (e.g., hydrochloric acid - HCl) – similar to the approach outlined by Bell and colleagues (2012) and delivered from small bioprocess bags (Labtainer, CX5-14 Single Web Film) using a small piezoelectric micro-pump (Takasago Electric, Inc.) contained within an oil-compensated housing. Dilute hydrochloric acid (0.1M) was added to the seawater stream at a flow of ~15 ml/min. This mixture of seawater and acid was homogenized by passing through a spiral static mixing cell (Stamixco HT-40-6.10-10-PTFE) before being routed to the membrane inlet (Figure 1).

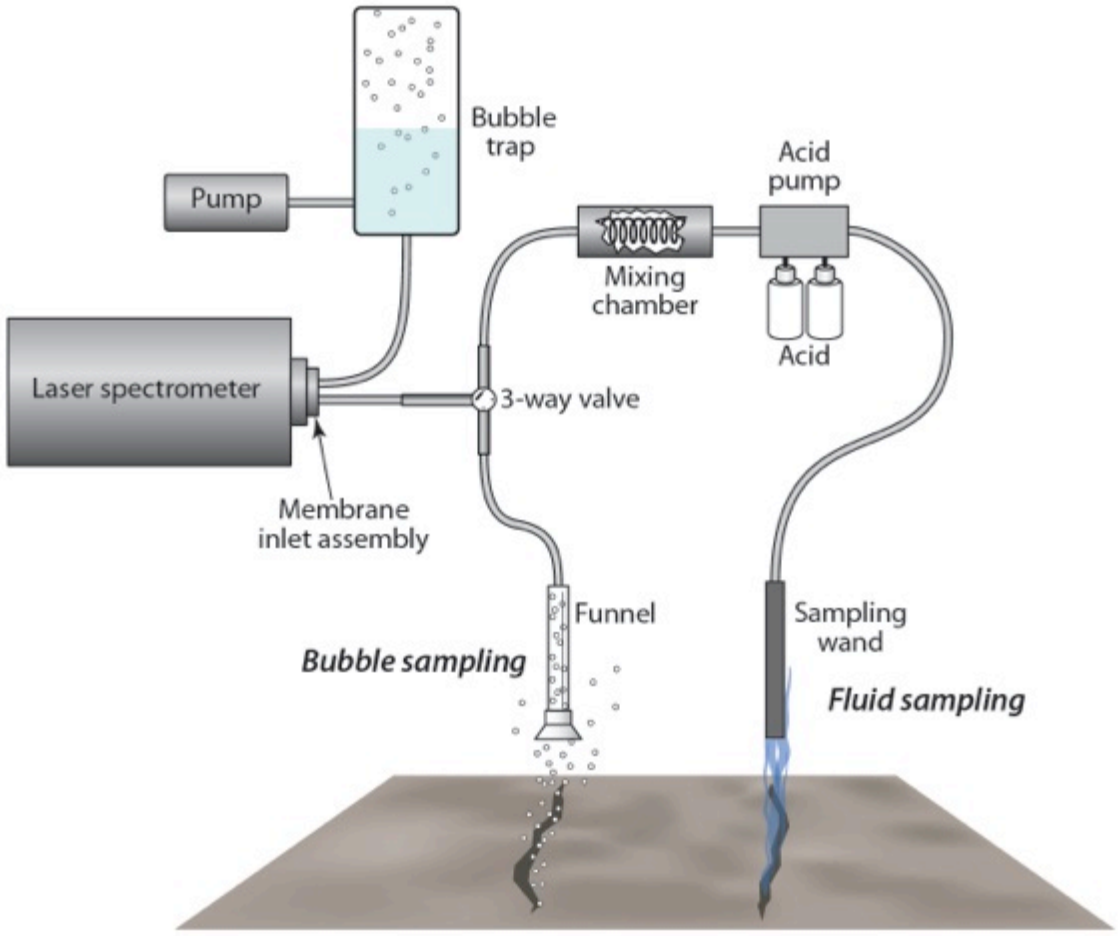

Fig. 1: Layout of fluid flowpaths and components integrated onto the ROV *Hercules*. A three-way valve was used for selection of fluid sampling or bubbling sampling. For fluid sampling, an acid pump coupled to a mixing chamber was used to acidify the seawater by adding dilute hydrochloric acid to the seawater. Bubbles were collected with a funnel-shaped sampling wand and caught with a bubble trap after the membrane inlet to avoid having the fluid pump lose prime. By using the bubble trap, the impeller pump could be used to pull either fluids or bubbles past the membrane inlet.

In the gas-sampling mode, an inverted funnel-shaped wand was used to capture bubbles rising from the sea floor with the impeller pump switched off (Figure 2). Once ~200-300ml of gas had accumulated in the funnel, the pump was switched on, pulling fluid through the sample lines and directing the gas sample past the membrane inlet. Downstream of the membrane inlet, sample bubbles were captured in a large bubble trap (internal volume of 3.1 L) in order to maintain prime of the impeller pump. The gas collected in the bubble trap was periodically released through the use of the ROV manipulator as needed. A fluid flow indicator, visible via ROV camera, was used to visually confirm flow through the tubing.

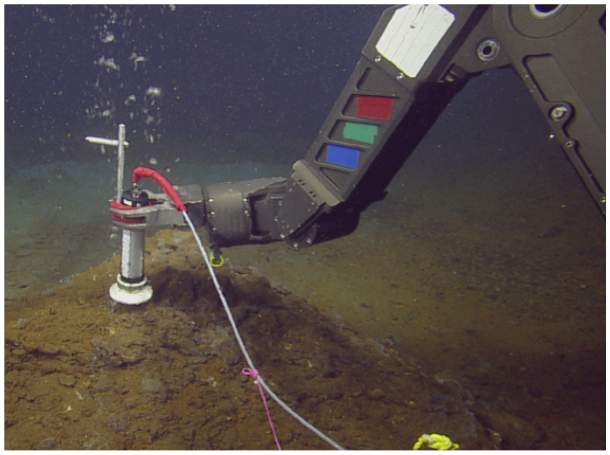

Fig. 2: Bubble collection was achieved by using a funnel attached to a sampling line that allowed bubbles to be pumped passed the membrane inlet. The ROV manipulator was used to place the funnel over bubble streams. (Image: Ocean Exploration Trust)

During sampling of gas bubbles, the length of time allowed for gas transfer across the membrane (normally 2-3 min for extraction of dissolved gases from fluids) was reduced to less than 5 seconds, as gas phase transfer under these hydrostatic pressures was greatly accelerated. While dissolved gas transfer across the membrane generally results in accumulation of 3-10 Torr of pressure inside the analyzer, >100 Torr was accumulated in only a few seconds while sampling gas bubbles. During dissolved gas sampling, the volume behind the membrane effectively equilibrates with the total partial pressure of dissolved gases at ocean depth, which is generally close to the partial pressure set during ventilation of deep water with the atmosphere or ~1 atm. In contrast, the total pressure of gases inside bubbles at depth is a function of the hydrostatic pressure at depth, and therefore equilibration across both sides of the membrane results in the increased transfer of gas into the analyzer.

2.4 Spectral Data and Fitting and Calibration

The spectral data of CH_4 was post-processed using a chemometric approach with basis sets of reference spectra made under controlled conditions (temperature and pressure) as detailed previously having a reported internal precision of ±0.8‰ (Wankel et al., 2013). The spectral data of CO_2 was post-processed using Voigt fits and data from the HITRAN database (Rothman et al. 2013) with isotopic species fit individually. Based on repeated analyses of a known CO_2 standard under laboratory conditions, we report here an internal precision of ±0.7‰, at internal concentrations of 10,000 ppm CO_2. Calibration gases (2500 ppm CH_4 ($\delta^{13}C_{CH4}$ = -40.1‰) and 10,000 ppm CO_2 ($\delta^{13}C_{CO2}$ = -10.7‰); Mesa Specialty Gases & Equipment) contained within the instrument were used for regular normalization throughout the course of the deployment. Carbon isotopic composition of these gases was determined at WHOI using either a ThermoFinnigan DeltaPlus isotope ratio mass spectrometer (IRMS) coupled to a HP 6890 gas chromatograph with a 30 m, 0.32 mm internal diameter AT-Q (Alltech) column or by direct injection onto a 30m, 0.32 mm internal diameter PorapPLOT Q (Supelco) column coupled to an Isoprime 100 isotope ratio mass spectrometer.

In addition to normalizing each sample analysis to an immediately preceding analysis of reference gas, the determination of sample $\delta^{13}C_{CO2}$ also requires correction for any isotopic fractionation occurring during extraction of CO_2 through the membrane [for CH_4 this was shown to be invariant over temperature and hydrostatic pressure, though sensitive to flow rate past the membrane (Wankel et al. 2013)]. For this deployment, however, we also collected independent fluid samples for lab-based analysis – offering an independent external benchmark for evaluating this first time effort for $\delta^{13}C_{CO2}$ analyses.

2.5 Collection of Independent Fluid Samples

In an effort to corroborate and validate the *in situ* isotope measurements, collection of independent fluid samples for lab-based measurement using conventional isotope ratio mass spectrometry was also conducted. Sample fluids were pumped using the same SBE-5M impeller pump, connected to a manually actuated valve manifold, which allowed sample fluid flow to be directed into bioprocess bags (Labtainer, CX5-14 Single Web Film) connected using a combination of 1/8" PEEK tubing and ¼" nylon tubing. Approximately 400-500ml of sample was allowed to fill the previously evacuated bags before being isolated by the valve manifold. The valve manifold was setup to allow continuous fluid flow and minimal cross-contamination of samples. Upon ascent, samples generally exhibited some degassing noted by the gas phase headspace in the bags. On deck, the fluid and headspace were shaken vigorously and headspace subsamples were rapidly transferred into previously evacuated 70ml serum vials before being stored at 4˚C. The samples were then analyzed for $\delta^{13}C$ composition of both CO_2 and CH_4 at WHOI by IRMS.

3. Study Site Description: Kick 'Em Jenny Submarine Volcano

Deployment of the described analytical system was conducted in September 2014 aboard the E/V *Nautilus* during cruise NA054 (Dive #1382) to the crater of the KEJ Volcano off the northwest coast of the Caribbean island of Grenada (Figure 3). KEJ lies at the southern end of the Lesser Antilles volcanic arc, formed as the result of the subduction of the South American Plate under the Caribbean Plate. KEJ is the most active volcano in the West Indies, with at least twelve recorded eruptions since 1939 (Lindsay et al., 2005). Based on visual observations by an investigatory expedition in 2013 to the KEJ crater (also with E/V *Nautilus*), our *in situ* isotopic investigation and analyses were targeted toward previously identified sites of active venting, located along the floor of the inner crater at a depth of ~265m. In addition to these primary focused flow sites, Shrimp Vent and Champagne Vent, a number of diffuse flow venting sites were also observed and investigated using the isotope analyzer and/or other sampling approaches. A detailed description of the KEJ volcanic system and its features has been reported by Carey and colleagues (2016).

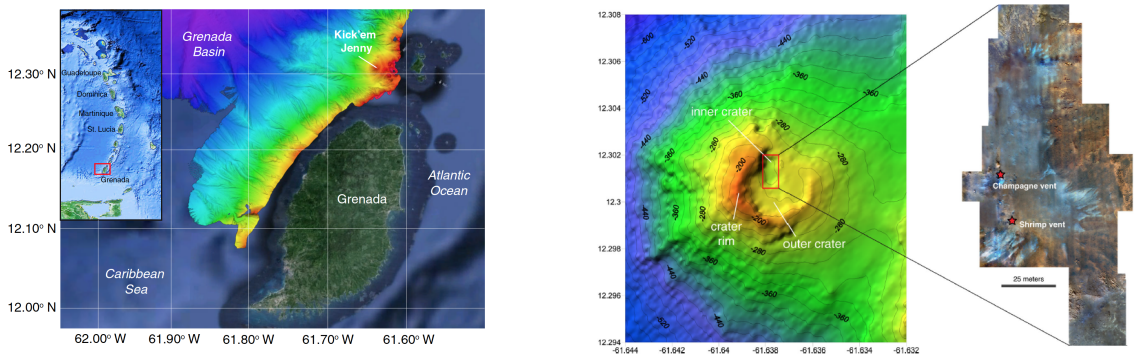

Fig. 3: Maps of Kick'em Jenny Volcano showing the geographical location (left) and bathymetry (right). Reprinted with permission from (Carey et al. 2016)

4. Use of Telepresence

The deployment and operation of the laser spectrometer system described above was conducted in part through the use of telepresence – the direct two-way linking of audio and video feeds from the ship and ROV to a shore-side operations base via a broadband satellite connection. Telepresence-enabled operations increase cruise participation by a broad and diverse audience including scientists ashore, students (Stephens et al. 2016), postdocs, educators and the general public. Importantly, this capability allows shore-based scientists to play integral roles in cruise and scientific exploration in real time. E/V *Nautilus* is equipped with telepresence capabilities (Bell et al. 2015), which were used for direct collaboration and communication between scientists on the ship and other team members on shore. During this cruise, one scientist leading the laser spectrometer deployment was aboard the ship while the rest of the laser spectrometer science team was shore-based, at the Inner Space Center at the University of Rhode Island. This telepresence connection allowed direct audio communication between the scientist on the ship and the scientists ashore. In

addition, through the use of the video link, the scientists ashore could view the deep sea ROV HD video feed in real time as well as see the computer interface with the laser spectrometer (including laser settings, valve positions and sample spectra) in real time as analyses were being made of the deep sea fluid and gas samples. The utilization of telepresence during this deployment enabled more scientists to be involved, enabling direct communication between scientists ashore and the scientist shipboard. The key disadvantage to having only one scientist shipboard is that it leaves one person solely responsible for 1) all technical components of the laser spectrometer including any necessary repairs, 2) running the instrument during all dives, and 3) preparing the instrument for redeployment between ROV dives. While telepresence enabled virtual participation in the dives, the physical participation was limited to the sole scientist shipboard.

5 Results

5.1 Laboratory Calibration of CO_2 Isotopic Fractionation

As designed, the larger surface area increased the gas flux across the membrane, decreasing the time needed for the gases to diffuse across it. Laboratory experiments designed to evaluate the carbon isotopic fractionation of dissolved CO_2 during extraction through the membrane inlet showed that, in contrast to the previous observations for methane extraction (Wankel et al. 2013), CO_2 exhibits a smaller carbon isotope fractionation when passing through the membrane (e.g., a smaller difference between true and measured $\delta^{13}C$ values). Figure 4 shows the difference between the $\delta^{13}C$ value of DIC in seawater (acidified inline to pH < 3) as measured by the laser spectrometer relative to its true value as determined offline via IRMS. For the conditions evaluated, results suggest that CO_2 passing through the membrane has a $\delta^{13}C$ offset value that is approximately 4.4 ± 0.4‰ lower than its true value. No variation was observed over fluid flow rates ranging from 7 to 265 ml/min (Figure 4).

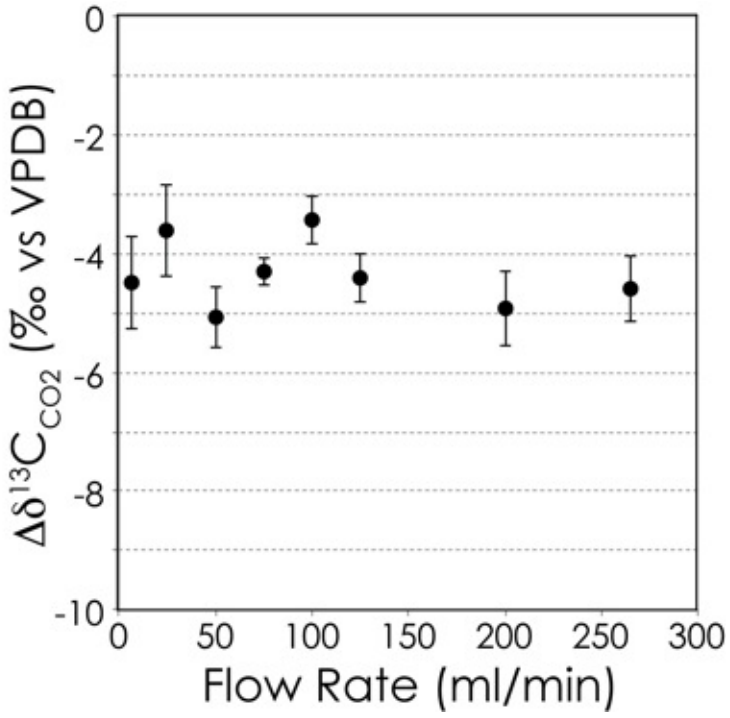

Fig. 4: Laboratory analysis of the difference between the actual $\delta^{13}C$ value of a DIC lab standard and the $\delta^{13}C$ value measured via laser spectroscopy using the membrane inlet over a range of flow rates. Flow rates during the actual deep-sea deployment to Kick'em Jenny were ~100ml/min.

5.2 Deployment Results

Two focused flow sites and two diffuse flow sites were investigated during the cruise (Table 1).

Table 1: Vent Site Characteristics

Vent Name	Location	Type	Depth (m)	Salinity (PSU) (from Carey et al. 2016)	Fluid Temperature (°C)
Shrimp	12°18.0564'N, 61°38.2740'W	Focused	262 - 263	Not reported	180^
Champagne	12°18.0762'N, 61°38.2710'W	Focused	263 - 264	36.160	160^
Neighbor	12°18.0508'N, 61°38.2700'W	Diffuse	261 - 263	Not reported	14 – 22
Fe-Oxide	12°18.0420'N, 61°38.2488'W	Diffuse	247 - 249	35.655	52 - 86

^maximum temperatures reported by Carey et al (2016).

5.2.1 General Site Observations

Within the inner KEJ crater, venting fluids and bubbles were analyzed using the *in situ* laser spectrometer (Figure 5). The two vigorously venting focused flow sites (Shrimp and Champagne) consisted of small mounds approximately 0.5 to 1 m in height and 2 - 3 m in diameter. In addition, diffuse venting fluids were measured or collected for analysis (Neighbor and Fe-oxide). Diffuse flow fluids emerged from small openings (<1-2 cm) scattered across the floor of the inner crater and generally exhibited far less bubble activity. Virtually all exposed surfaces in the vicinity of the venting sites were overlain by bright reddish-orange sediment (< 1 cm thick), consistent with high levels of iron oxides (Carey et al., 2016). Underneath these oxidized veneers gray/green/black sediments were observed, reflecting more reducing conditions consistent with microbial respiration/remineralization of sedimented organic matter. Associated with the areas of active focused venting, broad networks of whitish-yellowish bacterial mats were often observed, reflecting the hydrothermal delivery of reduced sulfur species (e.g., H_2S) and its oxidation by communities of sulfur oxidizing bacteria (Carey et al., 2016). These white mats were far smaller and less common near diffuse venting. Fluid sample collection generally targeted small open orifices where the highest temperatures were detected. At the main orifices of Shrimp and Champagne Vents fluid temperatures of up to 180 and 160˚C were recorded (~15cm into the vent orifice) (Carey et al., 2016). In comparison, fluid temperatures during sampling of the Neighbor and Fe-Oxide Vents were notably lower at 14-22˚C and 52-86˚C, respectively. Hydrothermal fluid venting was often closely associated with contemporaneous emissions of gas bubbles, with especially vigorous bubble release from the centermost orifice on the Champagne Vent mound. Carey and colleagues (2016) reported the highest volumetric gas fluxes from this centermost orifice at Champagne of approximately 2 L/min, with lower gas fluxes from Shrimp Vent reported to be ~0.5 L/min.

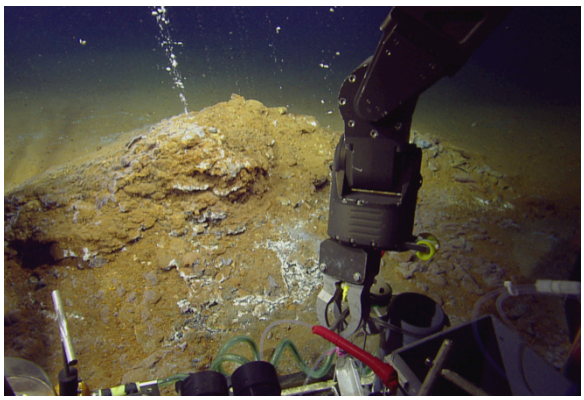

(a) Champagne Vent

(b) Shrimp Vent

Fig. 5: ROV images of the two focused flow vent sites, (a) Champagne and (b) Shrimp, investigated using the *in situ* laser spectrometer. Images courtesy of Ocean Exploration Trust.

5.2.2 *In situ* Analyses of Fluids and Bubbles

In the course of the 21 hour dive investigating hydrothermal venting within the KEJ inner crater, ~ 30 individual measurements (19 bubbles; 12 fluids) were made with the *in situ* laser spectrometer system. This number of measurements demonstrates the increased resolution that was immediately achievable using the system in this configuration, representing at least an order of magnitude more measurements (albeit of only one or two compounds) than would normally be achieved through collection of individual isobaric gastight samplers, which are often restricted to 2 - 4 per dive. To the best of our knowledge, these are the first reported *in situ* analyses of gas phase samples underwater.

Although submarine volcanic arc hydrothermal fluids are not known for containing high CH_4 concentrations, significant levels of CH_4 were regularly detected (Figure 6). Concentrations from the laser spectrometer are not robustly quantifiable due to the possible variation in the abundance of other major components of gas such as water vapor or nitrogen. However, comparison with the 2500 ppm standard gas suggests that KEJ fluids contained on the order of 1000-1300 ppm CH_4. This is consistent with levels detected by gastight sampling in 2013, which suggested CH_4 content between 500 to 2900 ppm (Carey et al 2016). By comparison, Figure 7 shows an example spectra for CO_2, clearly in high abundance and also consistent with gastight samples taken in 2013 (Carey et al. 2016), which suggested >90% CO_2 content. We were also able to directly detect hydrogen sulfide (H_2S), which was present in all of the volcanic gas bubble samples (Figure 7). We note that very little difference was observed between acidified fluids and unacidified fluids, consistent with the already low pH of the unacidified fluids (pH 4; Carey et al. 2016) and the corresponding dominance of carbonate speciation as CO_2.

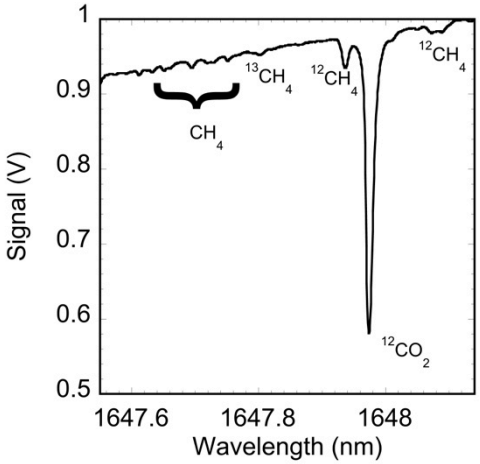

Fig. 6 Two isotopes of CH_4 ($^{12}CH_4$, and $^{13}CH_4$) along with $^{12}CO_2$ were detectable using a 1647 nm laser.

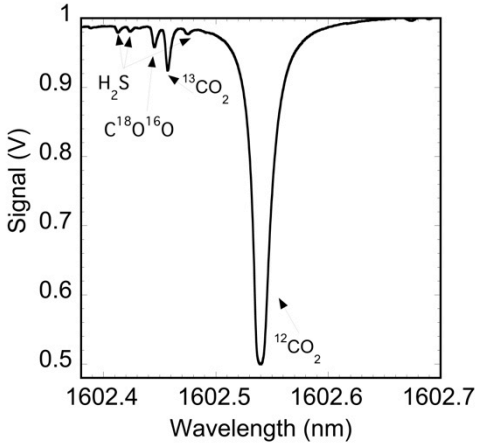

Fig. 7 Three isotopes of CO_2 ($C^{18}O^{16}O$, $^{12}CO_2$, and $^{13}CO_2$) along with H_2S were detectable using a 1602 nm laser.

5.2.3 Carbon Isotope Results for CO_2 and CH_4

Measured sample $\delta^{13}C_{CO2}$ and $\delta^{13}C_{CH4}$ values are first normalized to the internal standard reference gas and then adjusted for fractionation occurring during membrane extraction. Thus, the internally normalized 'raw' $\delta^{13}C_{CO2}$ values are adjusted by the experimentally determined membrane correction factor for $\delta^{13}C_{CO2}$ and $\delta^{13}C_{CH4}$, -4.4‰ and -8.3‰, respectively (see also, Wankel et al., 2013). Despite this correction, however, average $\delta^{13}C_{CO2}$ values from the fluid samples of Champagne Vent were still 10.0‰ higher than those determined by IRMS analysis of the independent fluid sample (Table 2; no further adjustment was required for $\delta^{13}C_{CH4}$ values). We therefore opted to use this IRMS based sample as our external benchmark and all reported $\delta^{13}C_{CO2}$ values below have been scaled by 10.0‰. Below we discuss possible explanations for this discrepancy (including non-linear error propagation for extremely high CO_2 levels, interference by H_2S, and influence of hydrostatic pressure on membrane fractionation for CO_2) as well as approaches for future designs to improve field accuracy in the absence of independent ground-truth analyses.

The $\delta^{13}C_{CO2}$ of samples from the focused flow fluids ranged from -5.7‰ up to -1.3‰ (Table 2). The average $\delta^{13}C_{CO2}$ value for fluids sampled at Champagne Vent (prescribed to the value of the IRMS analysis) was -4.8 ± 0.6‰, reflecting the mean of 4 samples (Table 2; Fig. 8). Gas phase bubble samples were measured at both Shrimp and Champagne Vents, averaging -3.6 ± 1.4‰ and -3.1 ± 1.9‰, respectively. The variability among these measurements made at each site reflects a combination of factors, including instrument precision, as well as variations in mixing between background seawater and vent fluid as sample gas is extracted during fluid pumping/sampling. Notably, fluid and bubble samples measured from the diffuse flow Neighbor vent exhibited markedly lower $\delta^{13}C_{CO2}$ values with an average of -10.7 ± 0.6‰ and -11.3 ± 0.9‰, respectively. Although no IRMS samples were collected from this diffuse flow site, the IRMS analysis of a sample collected from the other diffuse site (Fe-oxide) also yielded

a similarly low $\delta^{13}C_{CO2}$ value (-9.9‰; Table 2; Figure 8), lending some confidence to our adopted benchmarking approach. We acknowledge that ideally the sample collection would have been completed at the same location, yet we were limited in sampling capabilities and bottom time. We utilize the IRMS value here as a point of reference.

Where CH_4 levels were high enough for robust quantification (Wankel et al., 2013), $\delta^{13}C_{CH4}$ values are reported (Table 2). We note that spectral data were generally only resolvable on samples of Shrimp Vent, with average values of -30.3 ± 5.1‰ and -38.8 ± 2.3‰ for fluids and bubbles respectively. A single measurement made at Champagne yielded a value of -28.8‰, which was reasonably well corroborated by an IRMS value of -31.2‰.

Table 2: Measurements of carbon isotopic composition of CO_2 and CH_4 from hydrothermal fluids and bubbles sampled from sites within the inner crater of the Kick'em Jenny submarine volcano. Estimated external precision for laser spectrometer based $\delta^{13}C$ measurements is approximately ±1‰ for CH_4 and CO_2 (Wankel et al., 2013).

	Shrimp (focused)		**Champagne (focused)**		**Neighbor (diffuse)**		**Fe-Oxide (diffuse)**	
	Bubbles	Fluids	Bubbles	Fluids	Bubbles	Fluids	Bubbles	Fluids
$\delta^{13}C_{CH4}$	-41.4	-29.8	-28.8					
	-36.5	-32.0						
	-35.8	-38.0						
	-40.4	-24.8						
	-38.6	-26.9						
	-40.3							
$\delta^{13}C_{CH4}$ IRMS				-31.2				
$\delta^{13}C_{CO2}$	-4.3		-2.3	-4.8	-11.2	-10.0		
	-4.3		-1.3	-5.0	-11.7	-11.0		
	-4.2		-5.7	-5.1	-11.9	-11.0		
	-1.5			-3.8	-11.9			
					-9.8			
$\delta^{13}C_{CO2}$ IRMS				- 4.8				-9.9

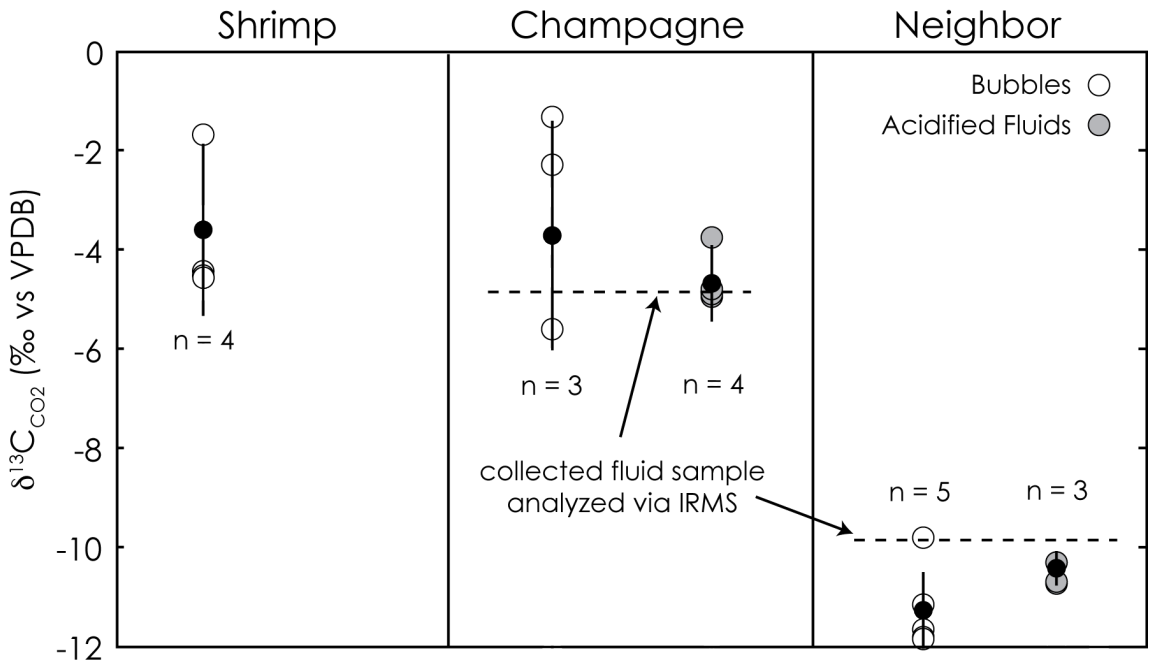

Fig. 8. $\delta^{13}C_{CO2}$ values measured by the laser spectrometer for the three inner crater venting sites (Shrimp, Champagne, and Neighbor) at Kick 'em Jenny. Measurements of bubbles are indicated as white circles, fluids as gray-shaded circles, and mean values as black-filled circles with lines denoting 1 standard deviation. The number of individual measurements is given as "n". Samples collected and then measured by IRMS are shown by dashed lines. Note that the IRMS value indicated for the Neighbor diffuse flow site was collected from a separate diffuse flow site (Fe-Oxide).

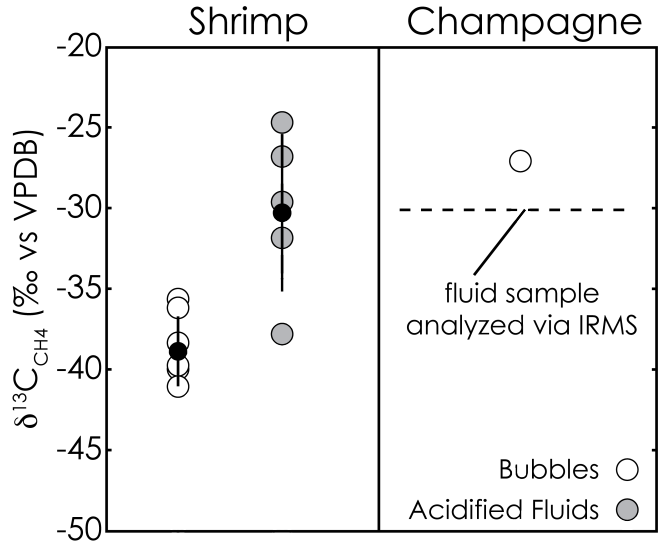

Fig. 9. $\delta^{13}C_{CH4}$ values measured by the laser spectrometer from two inner crater sites (Shrimp and Champagne Vents) at Kick'em Jenny. Measurements of bubbles are indicated as white circles, fluids as gray-shaded circles and mean

values shown by black-filled circles with lines denoting 1 standard deviation. The number of individual measurements are given as "n". A single fluid sample collected and measured by IRMS is indicated by the dashed line.

6.0 Discussion

6.1 Isotopic insights into subsurface processes at Kick'em Jenny

The development and deployment of an *in situ* laser spectrometer for combined carbon isotope analysis of CO_2 and CH_4 sheds new light on the nature of carbon fluxes at the KEJ submarine arc volcano. Mean $\delta^{13}C_{CO2}$ values for the KEJ vents exhibiting the largest fluid and gas fluxes (Champagne and Shrimp Vents) fall generally within the upper end of values found in other submarine hydrothermal systems (Fig. 10). Relative to $\delta^{13}C$ values of DIC in seawater (~0‰), fluids from sediment-associated ridge systems, such as Guaymas Basin for example, typically exhibit $\delta^{13}C$ values much lower than seawater CO_2 and DIC, reflecting the contribution of thermal degradation of organic matter to the total CO_2 fluxes (Seewald et al., 1994; Proskurowski et al., 2004; Welhan and Lupton, 1987). In comparison, $\delta^{13}C_{CO2}$ values in fluids from sediment-free mid-ocean ridge systems are usually higher than sediment-associated systems (-13 up to -4‰; Proskurowski et al., 2008; Merlivat et al., 1987; Welhan and Craig, 1983; Charlou et al., 2002), while fluids from volcanic arcs often exhibit values much closer to 0‰ (-2 to +1‰; Lupton et al., 2008; van Soest et al., 1998; Sano and Marty, 1995; Sano and Williams, 1996). The variation exhibited among these different hydrothermal vent systems directly reflects the relative contribution of CO_2 sources (e.g., thermal degradation of buried organic matter, magmatic CO_2, and outgassing of subducted carbon reservoirs including carbonate minerals and organic matter; Sano and Williams, 1996; Lupton et al., 2008). The co-emission of bubbles in active hydrothermal venting fluids found in volcanic arc systems appears to be a typical feature (Lupton et al., 2008; Carey et al., 2016), especially in comparison to venting at mid-ocean ridge systems, in which active venting of bubbles is almost never reported. In large part, this ebullition is thought to reflect the considerable input of magmatic degassing, with magmatic $\delta^{13}C_{CO2}$ thought to generally fall between -7 and -5‰ (Des Marais and Moore, 1984; Pineau and Javoy, 1983; Hoefs, 2010; Sakai et al., 1984). The higher $\delta^{13}C$ values typifying volcanic arc fluids reflect the additional contribution of carbon from the subducted oceanic crust, high in carbonate ($\delta^{13}C$ ~0‰) and having variable organic carbon content ($\delta^{13}C$ ~ -21 to -25‰) (Sano and Marty, 1995; Lupton et al., 2008). Thus, the values observed at the back arc KEJ volcano represent the mixture of carbon from mantle degassing together with release of carbon from carbonate sediments and organic matter during subduction of the South American Plate under the Caribbean Plate.

The significantly lower $\delta^{13}C_{CO2}$ values observed at the diffuse venting sites sampled along the southwestern and western edges of the inner crater (-9.8 to -11.9‰) clearly reflect some difference in the combination of processes contributing to carbon content of these fluids. Although sparse bubble emission

was observed at these diffuse venting sites (Neighbor and Fe-oxide), fluid emissions were significantly cooler than at the focused flow sites (Table 2). The sample collected for IRMS analysis from the Fe-oxide site contained considerably higher CH_4 (at least 4.5%), and much lower CO_2 than Shrimp/Champagne also reflecting a distinct compositional difference. Given the lower apparent fluid emission fluxes, cooler temperatures, elevation of CH_4 and lower $\delta^{13}C_{CO2}$ values we suggest that while the primary hydrothermal discharge appears to occur mainly at the Shrimp and Champagne Vents, these diffuse fluids have been influenced by a longer subsurface residence time, allowing for a greater influence by the pyrolysis of buried organic matter and possibly thermophilic anaerobic oxidation of CH_4 in the shallow subsurface. Making a few simple assumptions we can assess the feasibility that oxidation of subsurface organic matter or CH_4 is responsible for the lower $\delta^{13}C_{CO2}$ values seen in the diffuse venting sites. First we assume an endmember composition represented by the Shrimp/Champagne fluids of $\delta^{13}C_{CO2}$ = -4‰, a $\delta^{13}C_{CH4}$ = -41‰ and a $\delta^{13}C$ or buried organic matter of -21‰. Using these values in a simple mass balance, a $\delta^{13}C_{CO2}$ value in the diffuse fluids of -10‰ could be achieved if ~15% of the CO_2 derived from oxidation of subsurface CH_4 or if ~35% derived from oxidation of buried organic mater. While we cannot definitively determine the relative proportion of these processes, it appears evident that thermal degradation of buried organic matter, generating both CO_2 and CH_4, plays an important role in the carbon budget of these lower temperature diffuse venting sites. Although there is no direct evidence, it is also likely that some modest portion of the organic-derived CH_4 is oxidized to CO_2 before venting – presumably by anaerobic oxidation of methane (AOM). While AOM is usually considered coupled with the reduction of sulfate (here delivered through shallowly circulated seawater), the abundance of oxidized iron throughout the KEJ crater also raises the possibility that AOM may be, in part, coupled to reduction of iron oxide minerals (Beal et al., 2009; Wankel et al., 2012; Riedinger et al., 2014).

The $\delta^{13}C_{CH4}$ values of bubbles and fluids measured from the primary focused flow site (Shrimp Vent) fall generally within the range expected for thermogenically derived methane (-26.9 to -41.4‰; Table 2), which is methane derived from the thermal breakdown of organic matter, not by microbial methanogenesis (Whiticar, 1999). In general, there has not been wide reporting of $\delta^{13}C_{CH4}$ values from fluids of submarine back-arc systems. Co-registered $\delta^{13}C$ values of CH_4 and CO_2 may reflect high-temperature equilibrium processes (e.g., Horita, 2001; Tsunogai et al 1994) and/or low-temperature biologically catalyzed linkages between these pools (methane oxidation and/or methanogenesis; e.g., Proskurowski et al., 2008). While high subsurface temperatures can lead to isotopic equilibrium between magmatically-derived CO_2 and CH_4 (Horita, 2001; Tsunogai et al., 1994; Welhan, 1988), the corresponding values from Kick'em Jenny (Fig. 10) suggest temperatures (200 to 275˚C) which are higher than those observed, suggesting that the CH_4 and CO_2 are not in isotopic equilibrium. Furthermore, given the generally slow rates of carbon isotopic equilibration between CH_4 and CO_2 it is also unlikely that equilibration processes have

influenced CH_4 generated in the shallow subsurface. The apparently consistent offset between the $\delta^{13}C_{CH4}$ values in the bubbles and fluids (Table 2; Fig. 9) was somewhat unexpected and its explanation is not entirely clear. This observation may stem from differences in isotopic fractionation during membrane extraction of gas and dissolved phase CH_4, which was not explored in Wankel et al., (2013). Alternatively, this may reflect actual isotopic disequilibrium between dissolved and gas phase CH_4, arising from kinetic isotope fractionation as dissolved methane is stripped from solution by rising bubbles.

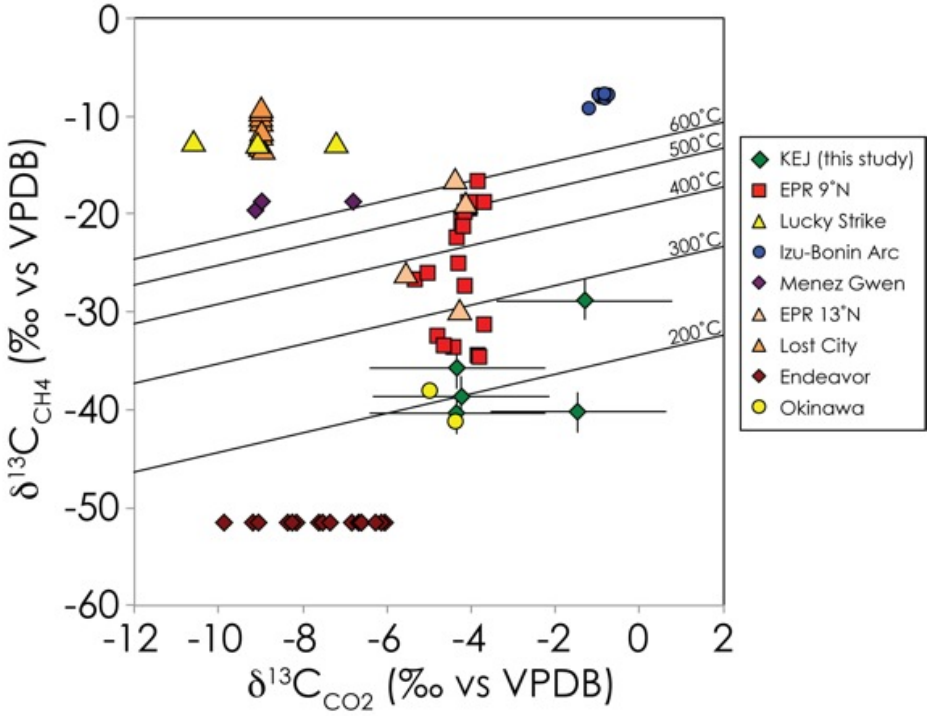

Fig. 10: Co-registered measurements of carbon isotopic composition of CH_4 and CO_2 measured by *in situ* laser spectrometer. Lines represent expected equilibrium relationship between CH_4 and CO_2 at indicated temperatures (Horita, 2001). Endmember compositions from other studies shown for comparison (EPR 9N (Proskurowski et al., 2008a); Lucky Strike and Menez Gwen (Charlou et al., 2002); Izu-Bonin Arc (Tsunogai et al., 1994); EPR 13N (Merlivat et al., 1987); Lost City (Proskurowski et al., 2008b); Endeavor Field (Proskurowski et al., 2004); Okinawa (Sakai et al., 1990).

The only previous investigation of CH_4 carbon isotopic composition in this area was reported by Koschinsky et al. (2007), showing CH_4 enrichments in the water column from the southwestern side of the KEJ crater at depths between 550 and 650m, having $\delta^{13}C_{CH4}$ values between -51 and -45‰, very close to values associated with air equilibrated CH_4 (-47‰). However, within these reported measurements, a significant trend of increasing $\delta^{13}C_{CH4}$ values with

higher concentrations was interpreted as reflecting mixing with a source having a considerably higher $\delta^{13}C_{CH4}$ value (>-45‰; Koschinsky et al., 2006), which would also be consistent with the higher $\delta^{13}C_{CH4}$ values we observed within the KEJ inner crater. However, it seems unlikely that the elevated CH_4 at depths of ~600m observed by Koschinsky et al. (2007) are linked to the fluids emanating from the inner crater (at ~260m). In particular, the elevated CH_4 samples collected by Koschinsky et al (2007) did not coincide with an observed ^3He isotopic anomaly associated more closely with shallower depths near the crater summit (200-300m). Together with the large biological communities observed in 2013 and 2014 (Carey et al., 2016) along the western margin of the volcano, it seems evident that the deeper water column source of CH_4 observed by Koschinsky et al (2006) was associated with the seepage of fluids from the volcano flank, and thus distinct from the CH_4 source we sampled from the inner crater.

6.2 Instrument Challenges, Successes, and Future Directions

The deep-sea laser spectrometer developed here was used to make 31 *in situ* isotopic measurements at both focused and diffuse flow sites, targeting both fluid and bubble analyses. A newly developed deep-sea bubble trapping approach allowed for the first time combination of *in situ* laser spectroscopy with sample stream acidification (for DIC) and direct measurement of bubble chemical/isotopic composition. This advance in deep-sea bubble analysis will have applicability to a variety of deep ocean environments, especially including the increasing detection of methane bubble emissions associated with methane hydrates and migration of hydrocarbon-rich geologic fluids (e.g., Skarke et al., 2014; Römer et al., 2012; Pohlman et al., 2009; Torres et al 2002).

The measurement variability using the laser spectrometer system as configured here stems both from the actual performance of the instrument as well as variability in the delivery of consistent sample. The sample is introduced to the laser spectrometer through a wand or funnel. The position of these (dictated by the ROV's ability to hold position and the pilot's ability to precisely place the sampling wand) together with other environmental changes (e.g. current shifts) influences the composition of the integrated fluid volume from which dissolved gases are being collected. As a result, background seawater may mix with the sample before it is collected, impacting isotopic measurements. Notably, the contribution of CH_4 from background seawater (low nM) can be largely dismissed. However, the contribution of DIC from mixing with background seawater may be substantial, depending on sampling conditions. Thus, interpretation of DIC isotope dynamics is limited by our inability to constrain this variable mixing of seawater and vent water while conducting *in situ* measurements. Future efforts will aim to combine deployments of the laser spectrometer with other *in situ* platforms sampling in the same sample stream. For example, combining *in situ* mass spectrometry (which measures continuously) would offer critical perspective on the composition of the time integrated sample being collected by the laser spectrometer, as well as provide

an independent assessment of concentrations of both isotopic analytes (CO_2 and CH_4) as well as other species – including those which might interfere with absorption spectroscopy.

As with the development of most technologies, challenges were encountered during this initial deployment to KEJ. Foremost, while high CO_2 levels from the volcanic fluids were anticipated, the relative amount of CO_2 introduced to the analyzer (through combination of the larger surface area membrane inlet, sample acidification and first-time *in situ* introduction of bubble samples) introduced more gas into the instrument than anticipated. For $\delta^{13}C_{CH4}$ analyses, the high relative levels of CO_2 noticeably influenced the ability to resolve $\delta^{13}C_{CH4}$, (see $^{12}CO_2$ peak in CH_4 spectra, Figure 6) requiring narrowing of the spectral window during post-processing to avoid potential artifacts. Similarly, $\delta^{13}C_{CO2}$ analyses of samples, which generally contained exceptionally high CO_2 levels relative to the internal reference gas may have suffered from error propagation when extrapolating $^{12}C/^{13}C$ values, perhaps giving rise to the discrepancy between calculated values and our benchmark field sample (see Section 4.2.3 above). Alternatively, this discrepancy may have been influenced by the presence of H_2S, in particular the presence of a H_2S spectral line under the primary $^{12}CO_2$ peak in the analyzed CO_2 region (not shown). Indeed from a theoretical standpoint, the contribution of H_2S to the $^{12}CO_2$ would lead to a decrease in calculated $\delta^{13}C$ values – which is at least consistent with the direction of the discrepancy between our calculated values and our the IRMS derived value. Moving forward, future efforts will continue targeting spectral regions that balance high sensitivity (e.g. line strength) with avoidance of such interfering species. In addition, we are working toward developing approaches for minimizing the accumulation of sample gas from the instrument at depth as well as using less gas for measurements (e.g., higher sensitivity, smaller internal volume).

Although our focus was on CH_4 and CO_2, the added ability to detect H_2S with the system also brings a new capability to dissolved and gas phase exploration in deep-sea settings where reduced sulfur compounds are often indicative of volcanic and/or microbial metabolic processes. In particular, H_2S is often only quantified by difference when samples are collected and analyzed for dissolved gas content. Thus, our approach suggests that future work should also begin exploring this analytical direction, which may provide important new insights into (bio)geochemical sulfur dynamics in deep ocean settings.

Funding:
This work was supported in part by grants to APMM and SDW from the NOAA Office of Ocean Exploration and Research (#NA14OAR011026), the National Science Foundation Ocean Technology and Interdisciplinary Coordination (OCE-1443683) and the Woods Hole Oceanographic Institution.

Acknowledgement
The authors thank the Captain, Crew, and Corps of Explorers aboard the E/V *Nautilus* (NA054) and the Ocean Exploration Trust (OET) for all of their support during the cruise both on the ship and at the Inner Space Center at the University of Rhode Island (URI). We would also like to thank the PIs, team members, and students of the NSF 'TREET' project for their valuable contributions, leadership, and watch standing through the NA059 cruise via telepresence. We are especially grateful to C. German (WHOI), K. Croff Bell (OET), S. Jasanoff (Harvard University), and A. Pallant (Concord Consortium) for their invitation to join the TREET project, as well as Expedition Leader C. Roman (URI), Lead Scientist and TREET Mentor S. Carey (URI), and TREET Mentor C. Van Dover (Duke University). We also thank S. Sylva (WHOI) for isotopic analyses in the laboratory, T. Lanagan (WHOI) for designing and building the bubble trap and M. Gupta, J.B. Leen and A. Fahrland (Los Gatos Research) for technical assistance throughout the project.

References

Baer, D.S., Paul, J.B., Gupta, M. and O'Keefe, A., 2002, September. Sensitive absorption measurements in the near-infrared region using off-axis integrated cavity output spectroscopy. In *International Symposium on Optical Science and Technology* (pp. 167-176). International Society for Optics and Photonics.

Beal, E.J., House, C.H. and Orphan, V.J. 2009. Manganese- and Iron-dependent Marine Methane Oxidation. *Science* 325, 184-187.

Bell, K.L.C., M.L. Brennan, and N.A. Raineault, eds. 2015. New frontiers in ocean exploration: The E/V *Nautilus* 2014 Gulf of Mexico and Caribbean field season. *Oceanography* 28(1), supplement, 60 pp., http://dx.doi.org/10.5670/oceanog.2015.supplement.01.

Bell, R.J., Short, R.T., Van Amerom, F.H. and Byrne, R.H., 2007. Calibration of an *in situ* membrane inlet mass spectrometer for measurements of dissolved gases and volatile organics in seawater. *Environmental science & technology*, *41*(23), pp.8123-8128.

Camilli, R. and Hemond, H.F., 2004. NEREUS/Kemonaut, a mobile autonomous underwater mass spectrometer. *TrAC Trends in Analytical Chemistry*, *23*(4), pp.307-313.

Camilli, R. and Duryea, A.N., 2009. Characterizing spatial and temporal variability of dissolved gases in aquatic environments with *in situ* mass spectrometry. *Environmental science & technology*, *43*(13), pp.5014-5021.

Carey, S., Olsen, R., Bell, K.L., Ballard, R., Dondin, F., Roman, C., Smart, C., Lilley, M., Lupton, J., Seibel, B. and Cornell, W., 2016. Hydrothermal venting and mineralization in the crater of Kick'em Jenny submarine volcano, Grenada (Lesser Antilles). *Geochemistry, Geophysics, Geosystems*, *17*, pp.1000-1019.

Charlou, J., Donval, J., Fouquet, Y., Jean-Baptiste, P. and Holm, N. 2002. Geochemistry of high H2 and CH4 vent fluids issuing from ultramafic rocks at the Rainbow hydrothermal field (36° 14'N, MAR). *Chemical Geology* 19, 345-359.

Des Marais, D.J. and Moore, J.G. 1984. Carbon and its isotopes in mid-oceanic basaltic glasses. *Earth and Planetary Science Letters* 69, 43-57.

Fietzek, P., Fiedler, B., Steinhoff, T. and Körtzinger, A., 2014. *In situ* Quality Assessment of a Novel Underwater p CO2 Sensor Based on Membrane Equilibration and NDIR Spectrometry. *Journal of Atmospheric and Oceanic Technology*, *31*(1), pp.181-196.

819 Graziani, S., Beaubien, S.E., Bigi, S. and Lombardi, S., 2014. Spatial and
820 temporal pCO2 marine monitoring near Panarea Island (Italy) using multiple low-
821 cost GasPro sensors. *Environmental science & technology*, *48*(20), pp.12126-
822 12133.
823
824 Hemond, H. and Camilli, R., 2002. NEREUS: engineering concept for an
825 underwater mass spectrometer. *TrAC Trends in Analytical Chemistry*, *21*(8),
826 pp.526-533.
827
828 Hodgkinson, J. and Tatam, R.P., 2012. Optical gas sensing: a review.
829 *Measurement Science and Technology*, *24*(1), p.012004.
830
831 Hoefs, J. 2010. Stable Isotope Geochemistry, 6th ed. Springer, Berlin-
832 Heidelberg.
833
834 Horita, J. 2001. Carbon isotope exchange in the system CO2-CH4 at elevated
835 temperatures. *Geochimica et Cosmochimica Acta* 65, 1907-1919.
836
837 Jost, H.J., Castrillo, A. and Wilson, H.W., 2006. Simultaneous 13C/12C and
838 18O/16O isotope ratio measurements on CO2 based on off-axis integrated cavity
839 output spectroscopy. *Isotopes in environmental and health studies*, *42*(1), pp.37-
840 45.
841
842 Koschinsky, A., Seifert, R., Knappe, A., Schmidt, K. and Halbach, P., 2007.
843 Hydrothermal fluid emanations from the submarine Kick'em Jenny volcano,
844 Lesser Antilles island arc. *Marine Geology*, *244*(1), pp.129-141.
845
846 Kosterev, A.A., Curl, R.F., Tittel, F.K., Gmachl, C., Capasso, F., Sivco, D.L.,
847 Baillargeon, J.N., Hutchinson, A.L. and Cho, A.Y., 1999. Methane concentration
848 and isotopic composition measurements with a mid-infrared quantum-cascade
849 laser. *Optics letters*, *24*(23), pp.1762-1764.
850
851 Lindsay, J.M., Shepherd, J.B. and Wilson, D., 2005. Volcanic and scientific
852 activity at Kick'em Jenny submarine volcano 2001–2002: implications for volcanic
853 hazard in the southern Grenadines, Lesser Antilles. *Natural Hazards*, *34*(1), pp.1-
854 24.
855
856 Lis, G., Wassenaar, L.I. and Hendry, M.J., 2008. High-precision laser
857 spectroscopy D/H and 18O/16O measurements of microliter natural water
858 samples. *Analytical Chemistry*, *80*(1), pp.287-293.
859
860 Lupton, J., Lilley, M., Butterfield, D., Evans, L., Embley, R., Massoth, G.,
861 Christenson, B., Nakamura, K.I. and Schmidt, M., 2008. Venting of a separate
862 CO2-rich gas phase from submarine arc volcanoes: Examples from the Mariana
863 and Tonga-Kermadec arcs. *Journal of Geophysical Research: Solid Earth*,
864 *113*(B8).

Martin, P.A., 2002. Near-infrared diode laser spectroscopy in chemical process and environmental air monitoring. *Chemical Society Reviews*, *31*(4), pp.201-210.

Merlivat, L., Pineau, F. and Javoy, M. 1987. Hydrothermal vent waters at 13˚N on the East Pacific Rise: Isotopic composition and gas concentration. *Earth and Planetary Science Letters* 84, 100-108.

McCurdy, M.R., Bakhirkin, Y., Wysocki, G., Lewicki, R. and Tittel, F.K., 2007. Recent advances of laser-spectroscopy-based techniques for applications in breath analysis. *Journal of Breath Research*, *1*(1), p.014001.

Penna, D., Stenni, B., Šanda, M., Wrede, S., Bogaard, T.A., Gobbi, A., Borga, M., Bonazza, M. and Chárová, Z., 2010. On the reproducibility and repeatability of laser absorption spectroscopy measurements for δ^2H and $\delta^{18}O$ isotopic analysis. *Hydrology and Earth System Sciences*, *14*(8), pp.1551-1566.

Pineau, F. and Javoy, M., 1983. Carbon isotopes and concentrations in mid-oceanic ridge basalts. *Earth and Planetary Science Letters*, *62*(2), pp.239-257.

Pohlman, J.W., Kaneko, M., Heuer, V., Coffin, R. and Whiticar, M. 2009. Methane sources and production in the northern Cascadia margin gas hydrate system. *Earth and Planetary Science Letters* 287, 504-512.

Proskurowski, G., Lilley, M.D. and Brown, T. 2004. Isotopic evidence of magmatism and seawater bicarbonate removal at the Endeaveor hydrothermal system. Earth and Planetary Science Letters 225, 53-61.

Proskurowski, G., Lilley, M.D. and Olson, E.J., 2008. Stable isotopic evidence in support of active microbial methane cycling in low-temperature diffuse flow vents at 9 50′ N East Pacific Rise. *Geochimica et Cosmochimica Acta*, *72*(8), pp.2005-2023.

Riedinger, N., Formolo, M., Lyons, T.W., Henkel, S., Beck, A. and Kasten, S. 2014. An inorganic geochemical argument for coupled anaerobic oxidation of methane and iron reduction in marine sediments. *Geobiology* 12, 172-181.

Römer, M., Sahling, H., Pape, T., Bahr, A., Feseker, T., Wintersteller, P. and Bohrmann, G. 2012. Geological control and magnitude of methane ebullition from a high-flux seep area in the Black Sea - the Kerch seep area. *Marine Geology* 319-322, 57-74.

Rothman, L.S., Gordon, I.E., Babikov, Y., Barbe, A., Benner, D.C., Bernath, P.F., Birk, M., Bizzocchi, L., Boudon, V., Brown, L.R. and Campargue, A., 2013. The

HITRAN2012 molecular spectroscopic database. *Journal of Quantitative Spectroscopy and Radiative Transfer*, *130*, pp.4-50.

Sakai, H., Des Marais, D.J., Ueda, A. and Moore, J.G. 1984. Concentrations and isotope ratios of carbon, nitrogen and sulfur in ocean-floor basalts. *Geochimica et Cosmochimica Acta* 48, 2433-2441.

Sano, Y. and Marty, B. 1995. Origin of carbon in fumarolic gas from island arcs. *Chemical Geology* 119, 265-274.

Sano, Y. and Williams, S.N. 1996. Fluxes of mantle and subducted carbon along convergent plate boundaries. *Geophysical Research Letters* 23, 2749-2752.

Seewald, J.S., Seyfried, W.E., Jr. and Shanks, W.C., III 1994. Variations in the chemical and stable isotope composition of carbon and sulfur species during organic-rich sediment alteration: An experimental and theoretical study of hydrothermal activity at Guaymas Basin, Gulf of California. *Geochimica et Cosmochimica Acta* 58, 5065-5082.

Sigrist, M.W., Bartlome, R., Marinov, D., Rey, J.M., Vogler, D.E. and Wächter, H., 2008. Trace gas monitoring with infrared laser-based detection schemes. *Applied Physics B*, *90*(2), pp.289-300.

Skarke, A., Ruppel, C.D., Modis, M., Brothers, D. and Lobecker, E. 2014. Widespread methane leakage from the seafloor on the northern US Atlantic margin. *Nature Geoscience* 7, 657-661.

Stephens, A.L., Pallant, A. and McIntyre, C., 2016. Telepresence-enabled remote fieldwork: undergraduate research in the deep sea. *International Journal of Science Education*, *38*(13), 2096-2113.

Tittel, F.K., Richter, D. and Fried, A., 2003. Mid-infrared laser applications in spectroscopy. In *Solid-State Mid-Infrared Laser Sources* (pp. 458-529). Springer Berlin Heidelberg.

Torres, M.E., McManus, J., Hammond, D.E., de Angelis, M.A., Heeschen, K.U., Colbert, S., Tryon, M.D., Brown, K. and Seuss, E. 2002. Fluid and chemical fluxes in and out of sediments hosting methane hydrate deposits on Hydrate Ridge, OR, I: Hydrologic provinces. *Earth and Planetary Science Letters* 201, 525-540.

Tsunogai, U., Ishibashi, J., Wakita, H., Gamo, T., Watanabe, K., Kajimura, T., Kanayama, S. and Sakai, H. (1994) Peculiar features of Suiyo Seamount hydrothermal fluids, Izu-Bonin Arc: Differences from subaerial volcanism. Earth and Planetary Science Letters 126, 289-301.

Van Soest, M.C., Hilton, D.R. and Kreulen, R., 1998. Tracing crustal and slab contributions to arc magmatism in the Lesser Antilles island arc using helium and carbon relationships in geothermal fluids. *Geochimica et Cosmochimica Acta*, *62*(19), pp.3323-3335.

Waechter, H. and Sigrist, M.W., 2007. Mid-infrared laser spectroscopic determination of isotope ratios of N2O at trace levels using wavelength modulation and balanced path length detection. *Applied Physics B*, *87*(3), pp.539-546.

Wahl, E.H., Fidric, B., Rella, C.W., Koulikov, S., Kharlamov, B., Tan, S., Kachanov, A.A., Richman, B.A., Crosson, E.R., Paldus, B.A. and Kalaskar, S., 2006. Applications of cavity ring-down spectroscopy to high precision isotope ratio measurement of 13C/12C in carbon dioxide. *Isotopes in environmental and health studies*, *42*(1), pp.21-35.

Wankel, S.D., Joye, S.B., Samarkin, V.A., Shah, S.R., Friederich, G., Melas-Kyriazi, J. and Girguis, P.R., 2010. New constraints on methane fluxes and rates of anaerobic methane oxidation in a Gulf of Mexico brine pool via *in situ* mass spectrometry. *Deep Sea Research Part II: Topical Studies in Oceanography*, *57*(21), pp.2022-2029.

Wankel, S.D., Germanovich, L.N., Lilley, M.D., Genc, G., DiPerna, C.J., Bradley, A.S., Olson, E.J. and Girguis, P.R. 2011. Influence of subsurface biosphere on geochemical fluxes from diffuse hydrothermal fluids. *Nature Geoscience* 4, 461-468.

Wankel, S.D., Adams, M.M., Johnston, D.T., Hansel, C.M., Joye, S.B. and Girguis, P.R. 2012. Anaerobic methane oxidation in metalliferous hydrothermal sediments: influence on carbon flux and decoupling from sulfate reduction. *Environmental Microbiology* 14, 2723-2740.

Wankel, S.D., Huang, Y.W., Gupta, M., Provencal, R., Leen, J.B., Fahrland, A., Vidoudez, C. and Girguis, P.R., 2013. Characterizing the distribution of methane sources and cycling in the deep sea via *in situ* stable isotope analysis. *Environmental science & technology*, *47*(3), pp.1478-1486.

Weidmann, D., Wysocki, G., Oppenheimer, C. and Tittel, F.K., 2005. Development of a compact quantum cascade laser spectrometer for field measurements of CO2 isotopes. *Applied Physics B*, *80*(2), pp.255-260.

Welhan, J.A. and Craig, H. 1983. Methane, hydrogen and helium in hydrothermal fluids at 21˚N on the East Pacific Rise, in: Rona, P.A., Bostroem, K., Laubier, L., Smith, K. (Eds.), *Hydrothermal processes at seafloor spreading centers* Plenum Press, New York, NY, USA.

Welhan, J.A. and Lupton, J.E. 1987. Light hydrocarbon gases in Guaymas Basin hydrothermal fluids: thermogenic versus abiotic origin. *American Association of Petroleum Geology Bulletin* 71, 215-223.

Welhan, J.A. 1988. Origins of methane in hydrothermal systems. *Chemical Geolgy* 71, 183-198.

Whiticar, M.J., 1999. Carbon and hydrogen isotope systematics of bacterial formation and oxidation of methane. *Chemical Geology*, *161*(1), pp.291-314.